

MuTool Final Report

Figures & Tables

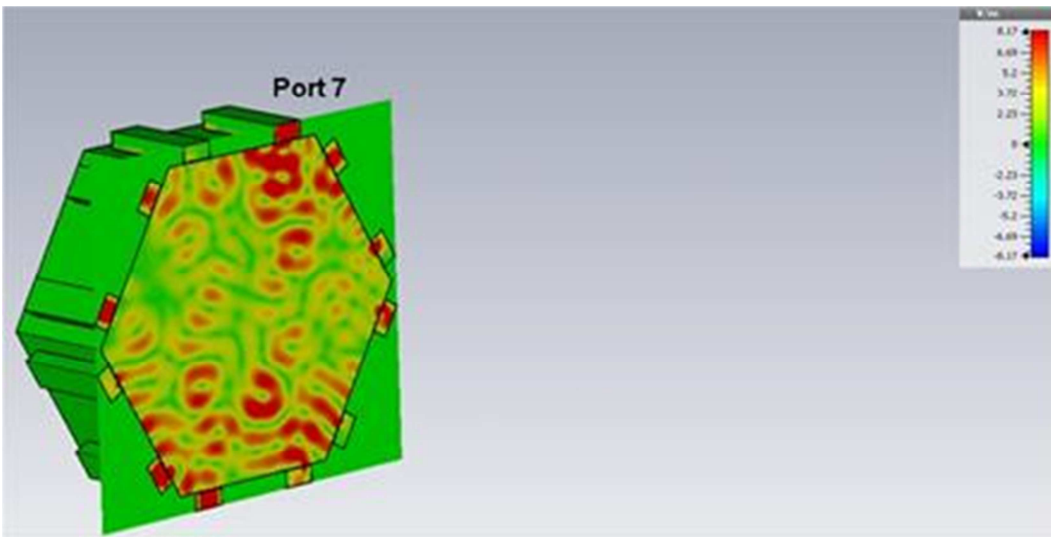


Figure 1: Distribution of electromagnetic field inside the microwave oven cavity. The absolute values of the E-field created by port 1 and 7 can be transferred to each other by a 180° rotation along the chamber's centre line.

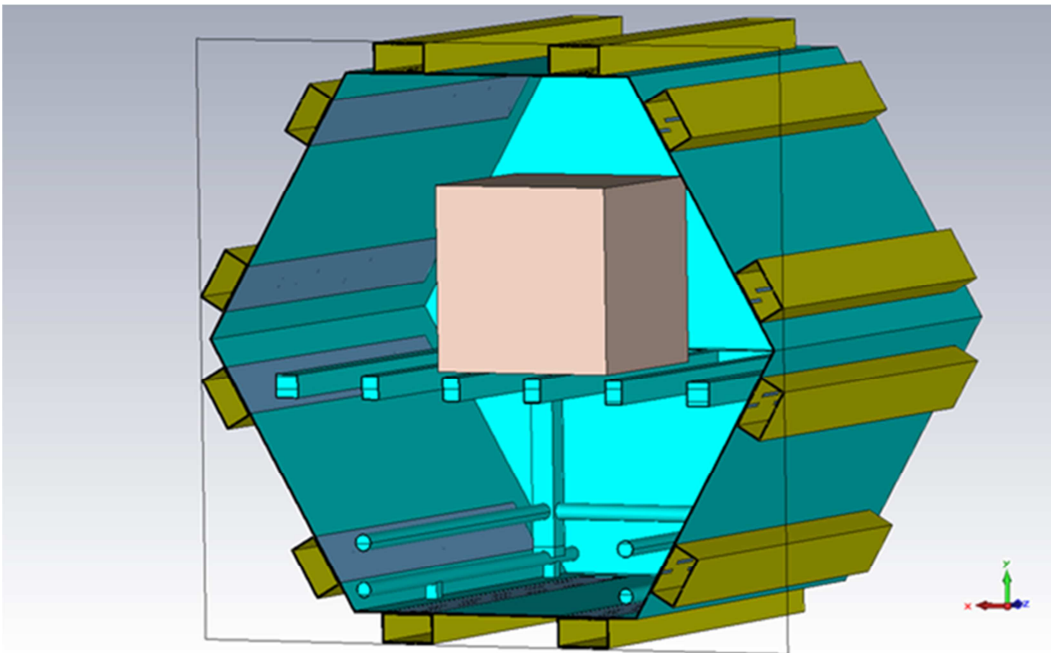


Figure 2: Cross sections of HEPHAISTOS chamber with integrated support bench and ceramic test tool.

MuTool Final Report

Figures & Tables

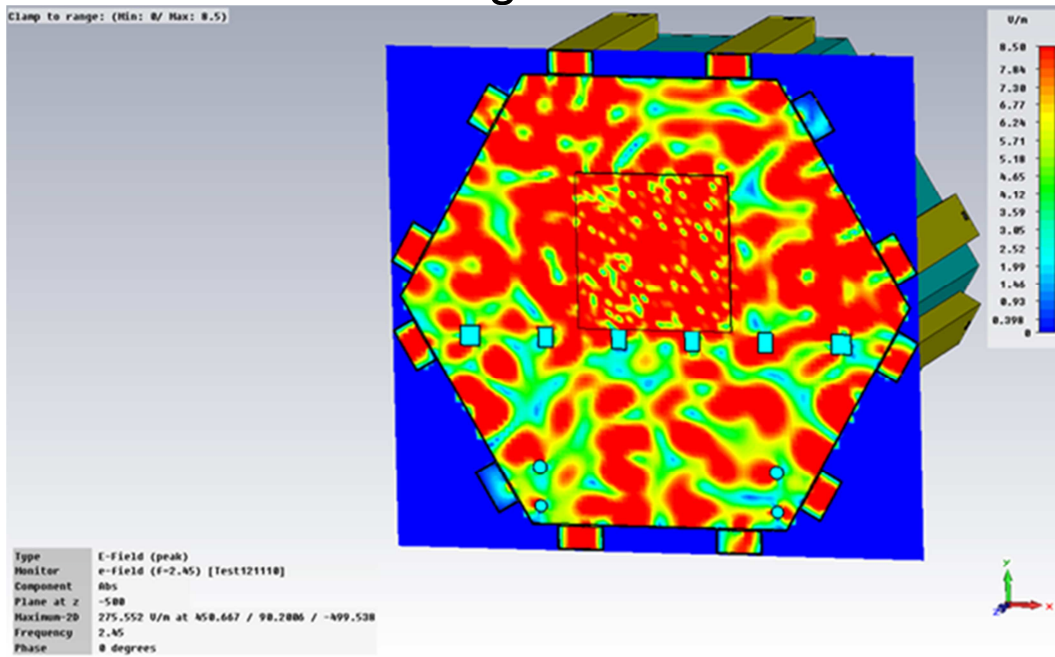


Figure 3: Cross sections of simulated absolute values of electrical field – Middle of Chamber. Note the homogenization effect of the field distribution within the Ceramic Test Tool

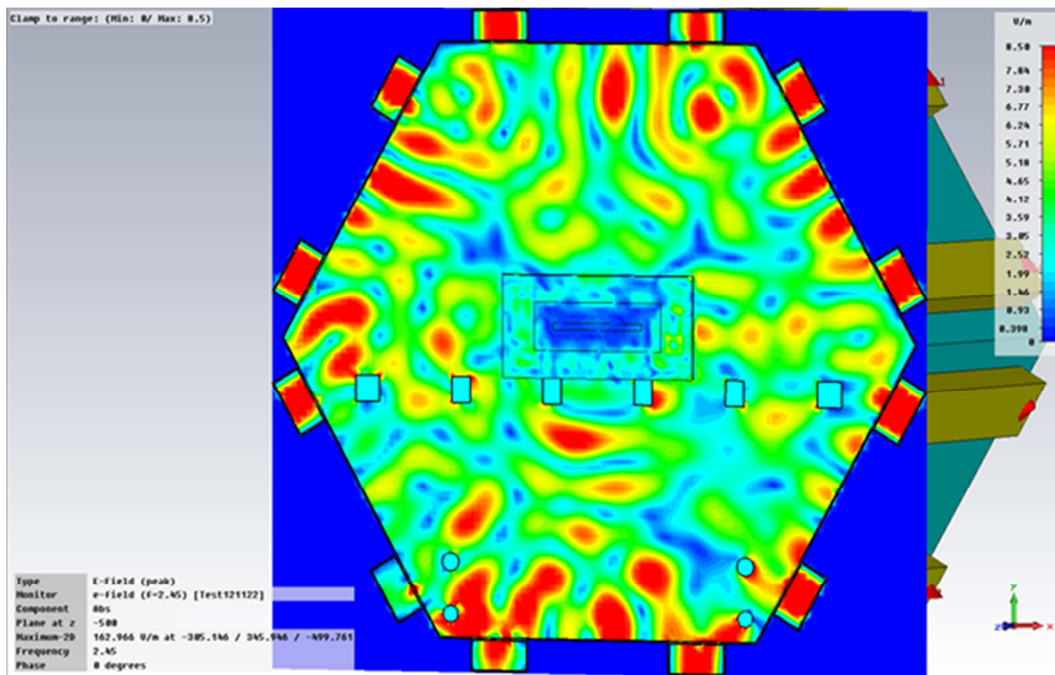


Figure 4: Cross sections of simulated absolute values of electrical field. Note the creation of the homogeneous bubble around the composite load area in the tool

MuTool Final Report

Figures & Tables

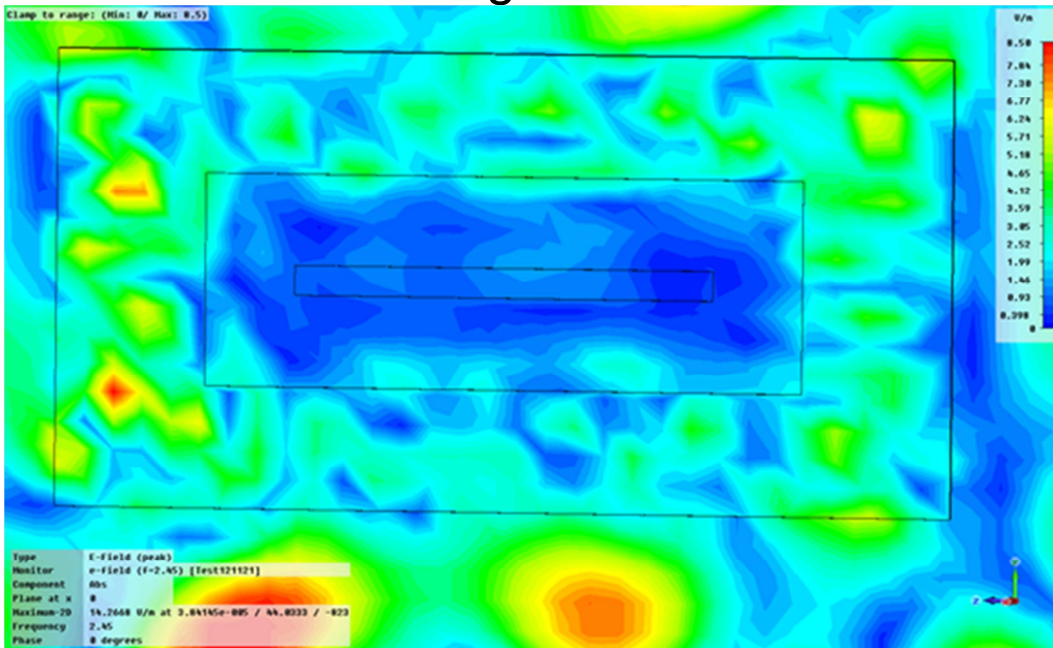


Figure 5: Close up of the tool from Figure 4: Detailed view on the empty composite load cross section – Note the homogeneity effect on the boundary of the tool – the absorption is created in the ferrite coated layer creating a temperature bubble.

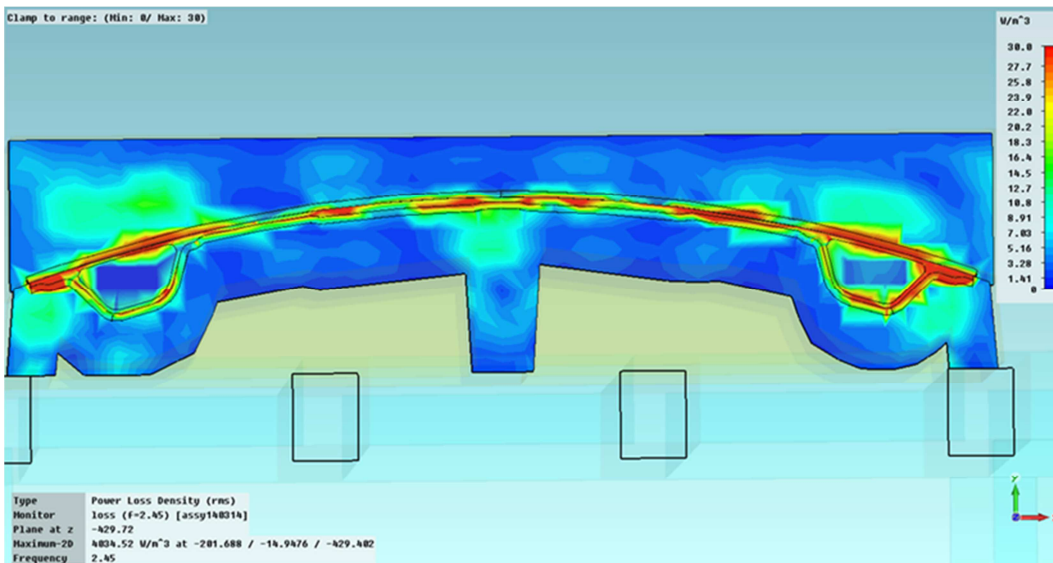


Figure 6: Simulation of prototype tool

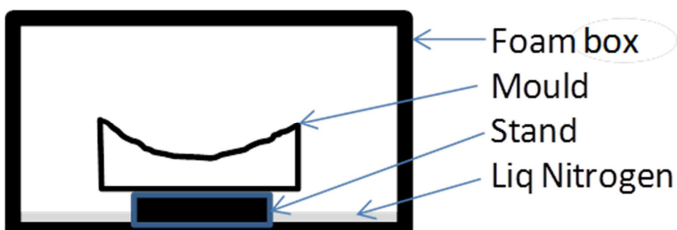


Figure 7: Freeze casting configuration

MuTool Final Report

Figures & Tables

Code	Sol volume (cm ³) ¹	Al ₂ O ₃ mass (g)	Ferrite mass (g)	Heating test	Comments
HS 40 (40% silica) sol in “cupcake” mould					
S1	60 (~76)	60	0	Yes	Sol-vol:Powder weight Ratio 1:1 Fluid slurry
S3	45	60	0	Yes	Sol-vol:Powder weight Ratio 1:1.3 Thixotropic slurry
S4	45	54	6 (10% w/w)	Yes	Good heating performance
S11	(54)	57	3 (5% w/w)	Yes	Effect of ferrite loading
S12	(54)	54	6 (10% w/w)	Yes	
S13	(54)	48	12 (20% w/w)	Yes	
S14	38 (50)	50	0	Yes	
S15	38 (50)	66.5	0	Yes	
1Ludox CL (30% silica) sol in “cupcake” mould					
S5	45	54	6	No	Did not freeze cast, melted when warmed
HS 40 (40% silica) sol in rectangle aluminium tool					
S6	150 (~190)	195		Yes	
S7	150	175	19.5 (10% w/w)	Yes	
S8 S	48 (63)	75	8.3	Yes	Bi-layer specimen with ferrite loaded surface
S8 B	97 (127)	142	0	Yes	
S18 S	60 (77)	90	10	No	Bi-layer specimen with ferrite loaded surface
S18 B	118 (154)	200	0	No	

Table 1: Composition of the different samples produced

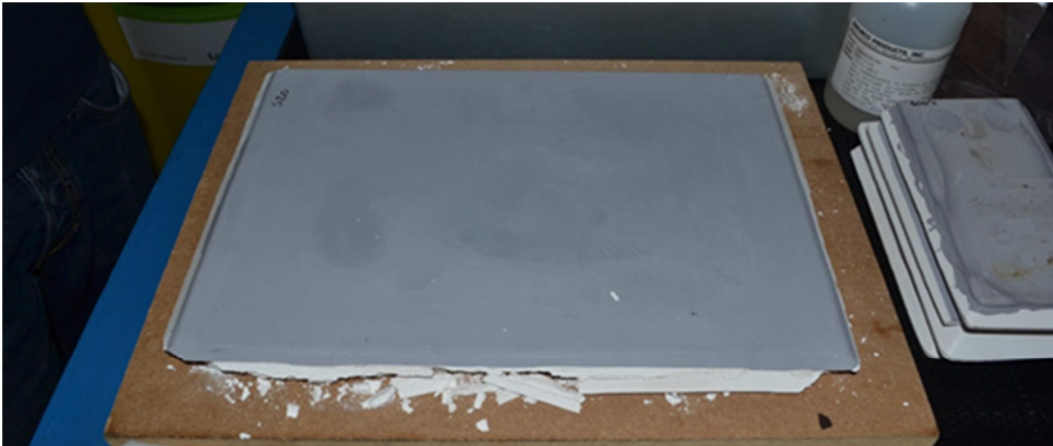
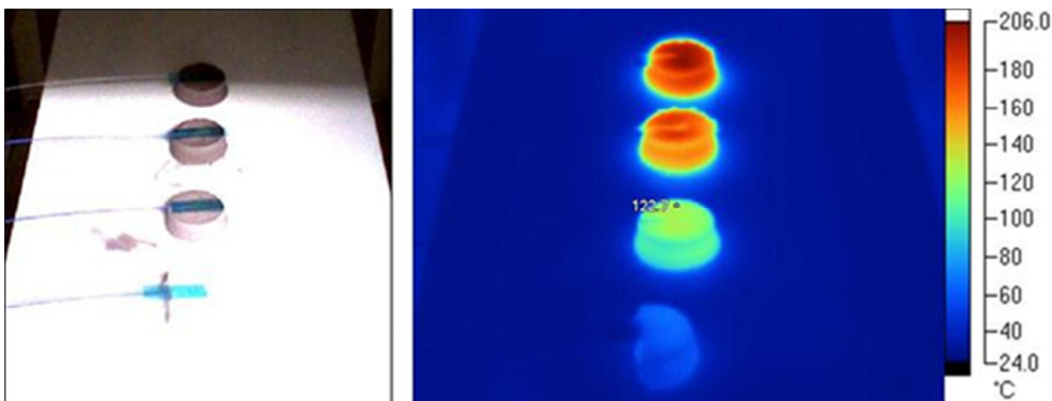


Figure 8: Freeze casting of flat specimens



¹ mass (g) is also given in parenthesis for some of the combinations

MuTool Final Report

Figures & Tables

Figure 9: Freeze casting specimens of cordierite with different amounts of ferrites in the mixture. The thermograph on the right shows the different levels of heating achieved.

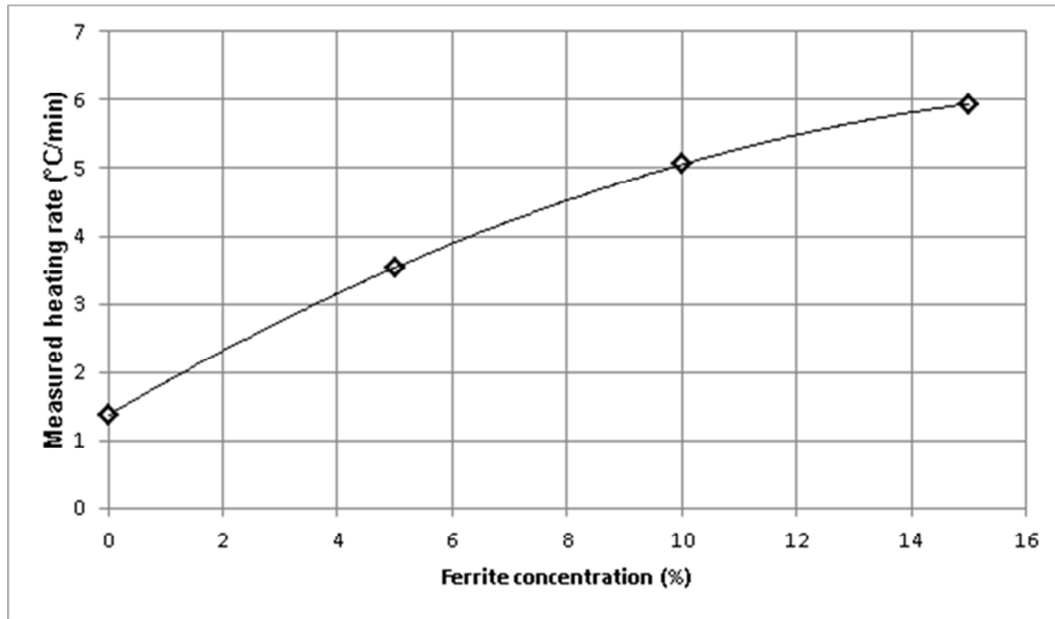


Figure 10: Dependence of the obtained heating rate on ferrite doped samples as a function of the ferrite loading

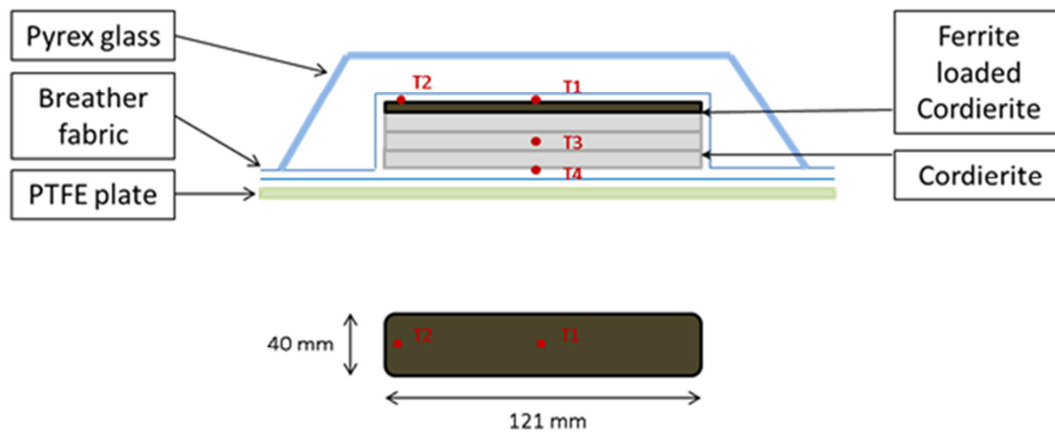


Figure 11: Experimental layout (top) and specimens dimensions (bottom). The location of the thermocouples is shown

Ferrite loading	Ferrite layer thickness (mm)									
	0		1.3		2.5		5		7.5	
	T_{\max} (°C)	r_{\max} (°C/min)	T_{\max} (°C)	r_{\max} (°C/min)	T_{\max} (°C)	r_{\max} (°C/min)	T_{\max} (°C)	r_{\max} (°C/min)	T_{\max} (°C)	r_{\max} (°C/min)
0 %	80	5								
15%			-		189	16.7	>225 ²	27.6	>220 ²	29.1
30%			92		216	19.0	>220 ²	179 ³	>242 ²	121 ³

Table 2: Experimental results from test of samples with variable ferrite layer thickness

² Temperature increase was too abrupt and the thermocouple stopped measuring. The test was terminated before the 10 minute interval

³ The temperature increase was too high. The ferrite specimen broke due to the induced thermal stresses

MuTool Final Report

Figures & Tables

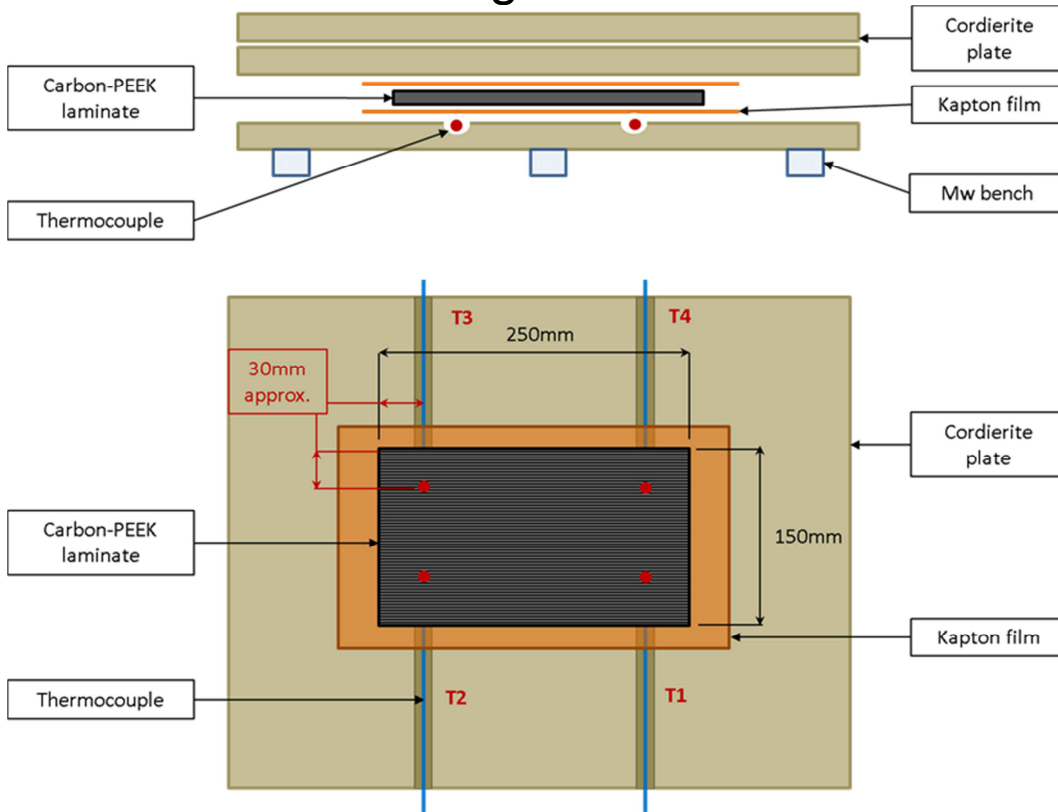


Figure 12: Initial set up chosen to process tests in the MW. On top view, red dots represent the tips of the thermocouples.

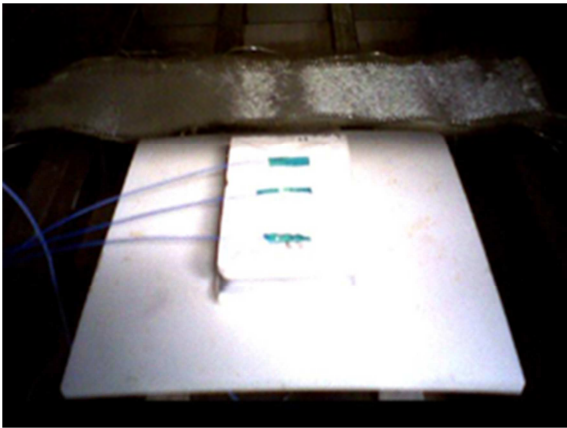


Figure 13: Tool layout after completion of the PEEK polymerisation reaction – top view.

MuTool Final Report

Figures & Tables

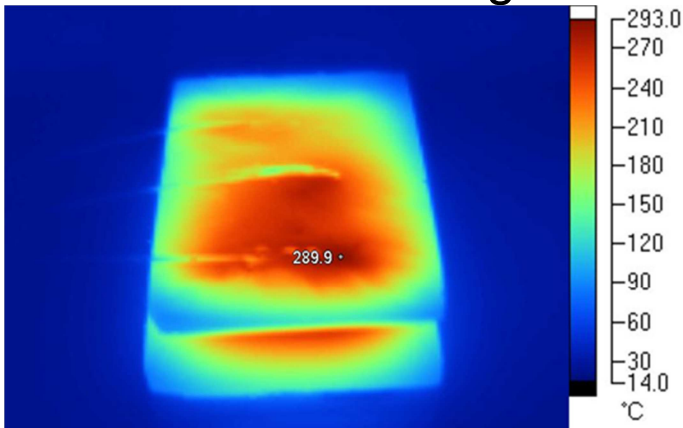


Figure 14: Thermal image of the tool after completion of the PEEK polymerisation reaction – top view



Figure 15: Tool layout after completion of the PEEK polymerisation reaction – side view

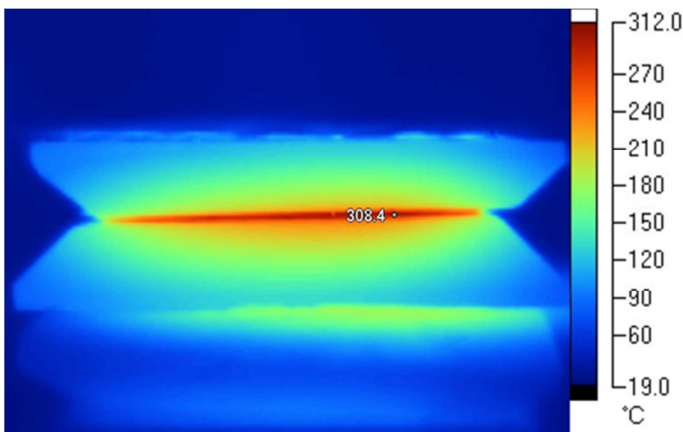


Figure 16: Thermal image of the tool after completion of the PEEK polymerisation reaction – side view

MuTool Final Report

Figures & Tables

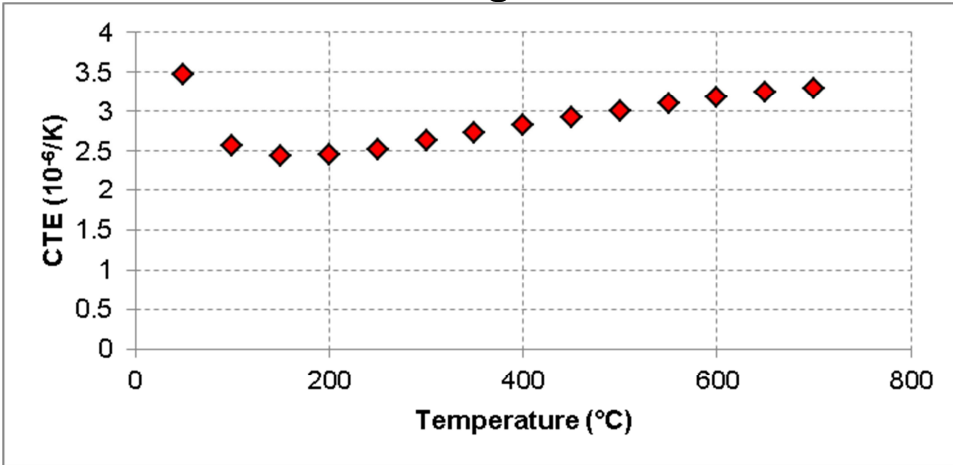


Figure 17: CTE evolution for cordierite ceramic

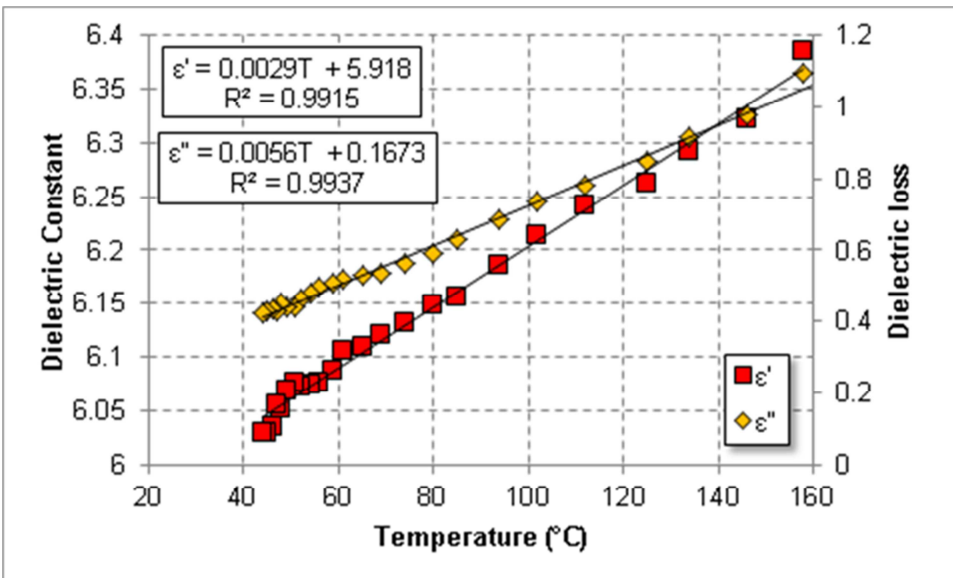
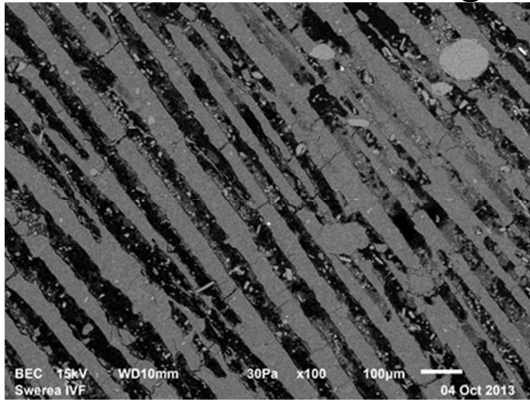


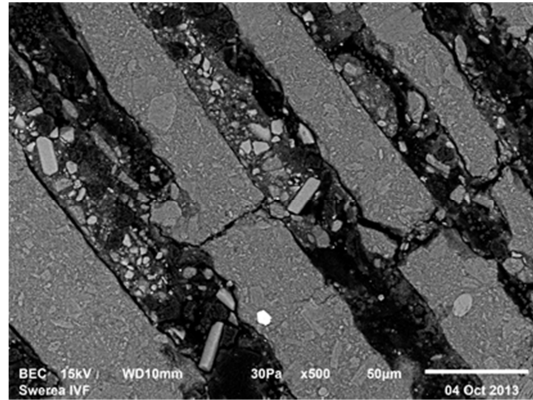
Figure 18: Dielectric constant and dielectric loss for 70% Cordierite – 30% Ferrite

MuTool Final Report

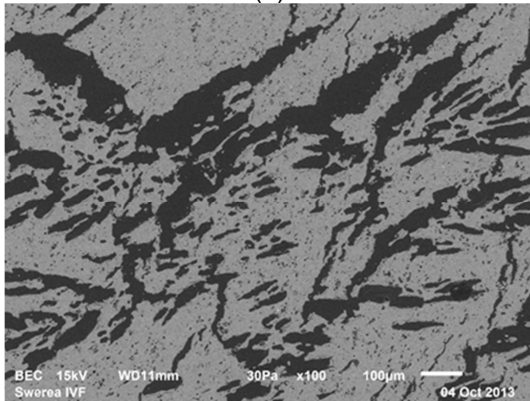
Figures & Tables



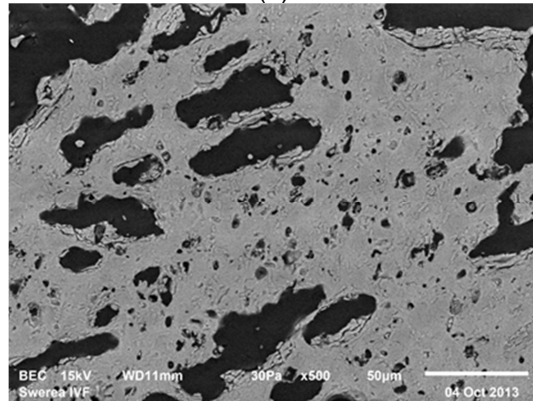
(a)



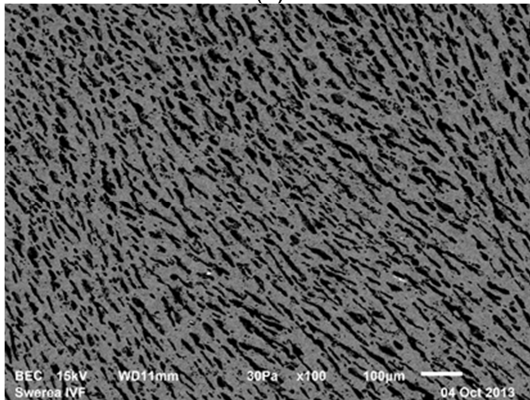
(b)



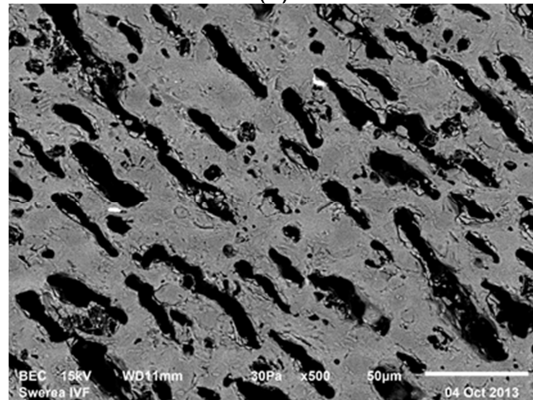
(c)



(d)



(e)



(f)

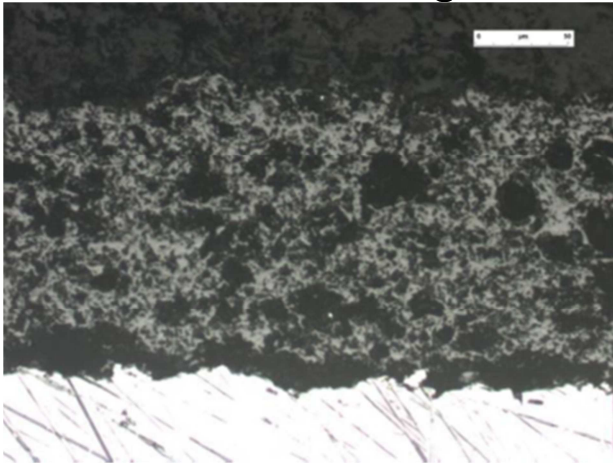
Figure 19: Microstructure of freeze cast and freeze dried materials. The dark areas are porosity and the light areas represent the ceramic material. Freeze cast and heat treated alumina (a, b), cordierite cast from a water based suspension with a solids loading of 50vol% sintered at 1200°C (c, d) and cordierite from a water-glycerol based suspension with a solids loading of 50vol% sintered at 1200°C (e, f).

Sample ID	Seed layer	Coating thickness (µm)	Coating Porosity (%)	Micro hardness (HV0.3)	Adhesion (MPa)
E130306/1-4	None	160	14.1	340	21
E130306/5-8	None	160	14.4	265	25
E130306/9-12	NiAl	218	5.7	431	32.5
E130306/13-16	None	206	10.1	463	35.5

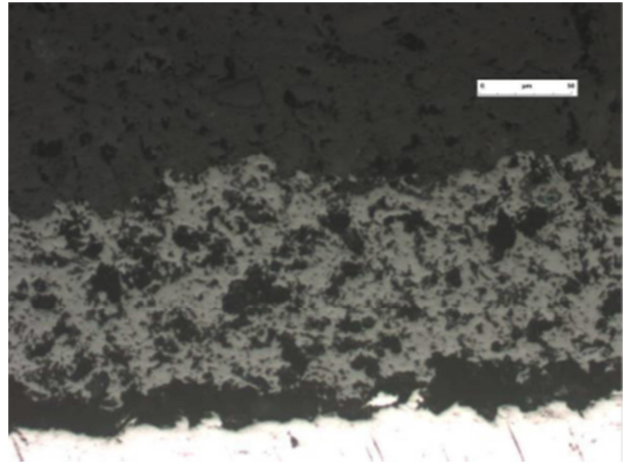
Table 3: Test results on thermal spraying of ferrite on metallic substrate

MuTool Final Report

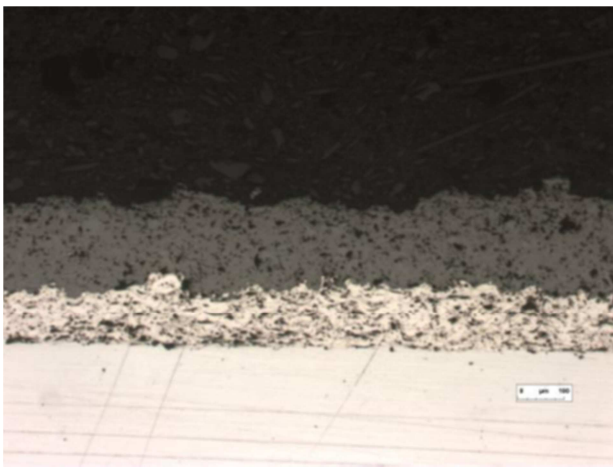
Figures & Tables



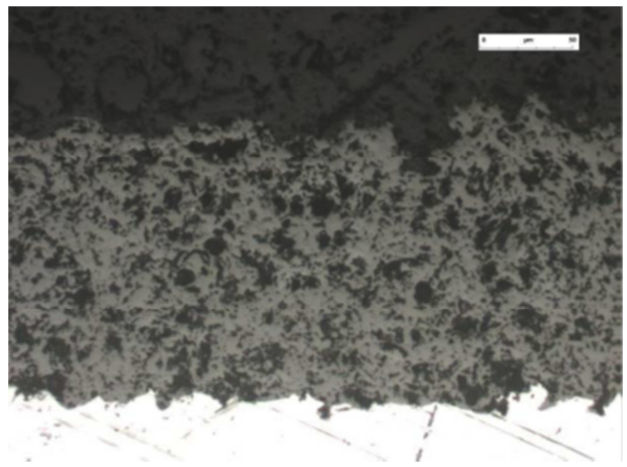
(a)



(b)



(c)



(d)

Figure 20: Microstructure of thermal spray of ferrite on metallic substrate: (a) E130306/1-4, (b) E130306/5-8, (c) E130306/9-12, (d) E130306/13-16

Sample ID	Seed layer	Coating thickness (μm)	Coating Porosity (%)	Micro hardness (HV0.3)	Adhesion (MPa)
E130417/1-4	None	400	5.9	500	20.5

Table 4: Test results on thermal spraying of ferrite on metallic substrate

MuTool Final Report

Figures & Tables

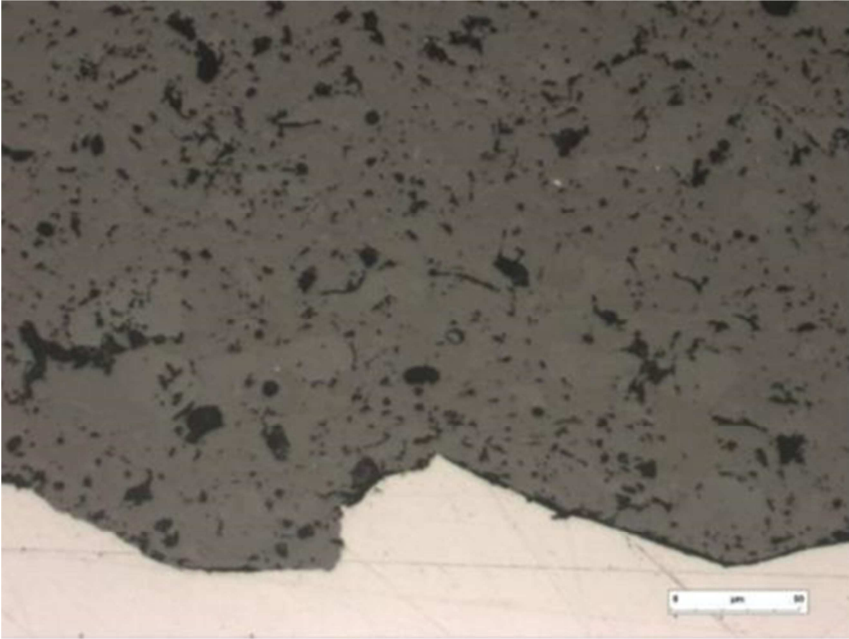


Figure 21: Microstructure of thermal spray of ferrite on cordierite substrate

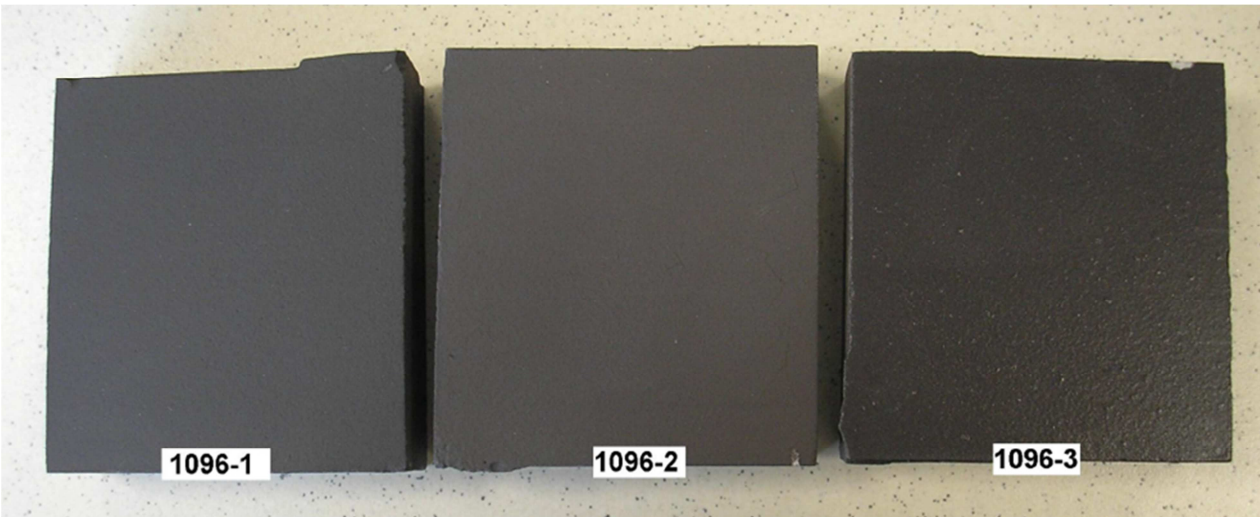


Figure 22: Glaze samples containing 25% w/w ferrite and different concentration of other constituents in order to reduce the thermal mismatch between the ferrite and cordierite. The sample numbers are shown.

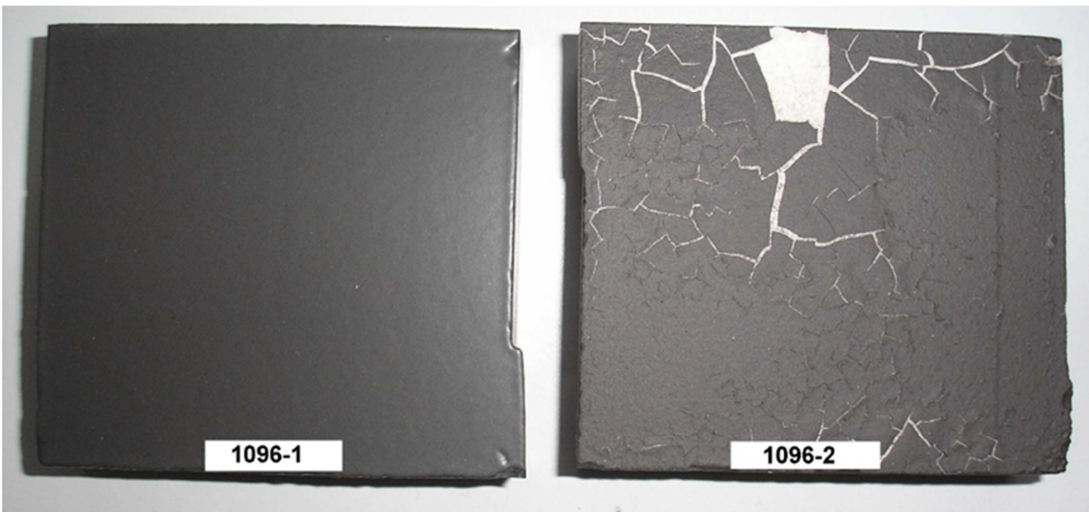


Figure 1: Glaze samples after second firing at 1100°C

MuTool Final Report

Figures & Tables

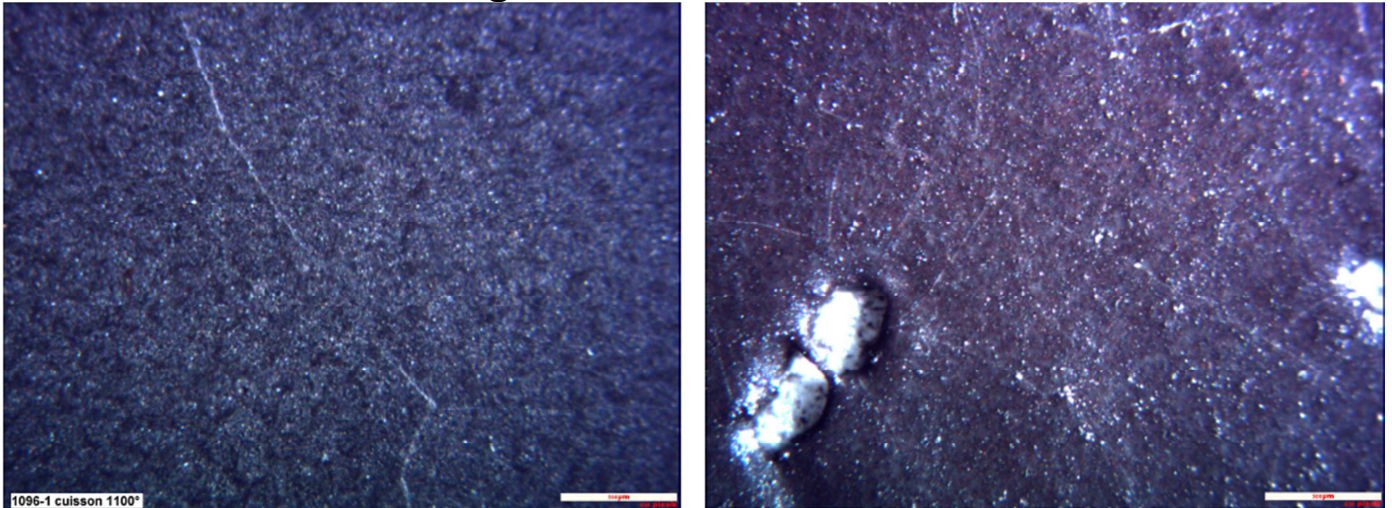


Figure 2: Optical microscopy images of samples 1096-1 (left) and 1096-3 (right) after the second firing at 1100°C and 1050°C respectively

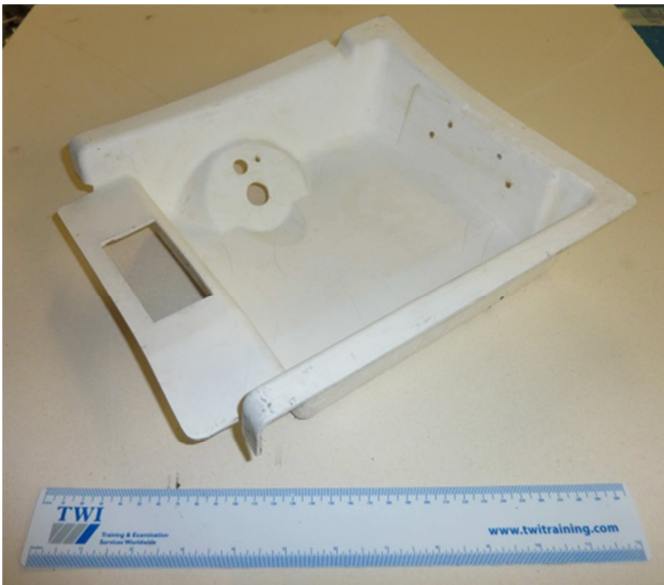



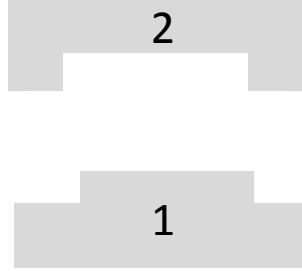


Figure 25: Sample part supplied by Microcab

 <p>Figure 3: Schematic for the construction of the plug tool</p>	 <p>Figure 4: Plug tool de-moulded</p>	 <p>Figure 5: Construction of the cavity tool</p>	 <p>Figure 6: Schematic of final plug and cavity tools</p>
------------------------------------------------------------------------------------------------------------------------------------------------------	---------------------------------------------------------------------------------------------------------------------------	---------------------------------------------------------------------------------------------------------------------------------------	-------------------------------------------------------------------------------------------------------------------------------------------------

MuTool Final Report

Figures & Tables

Table 1: Solutions quantities for the fabrication of the plug and cavity tools

Product	Plug tool	Cavity tool
Sol ⁴ (lt)	3	2.2
Sol (g)	3900	2860
Out of which water (g)	2340	1716
Out of which silica (g)	1560	1144
Glycerol (g)	30	20
Al ₂ O ₃ fibre (g)	150	150
Al ₂ O ₃ powder (g)	7000	5000
Total weight of the mixture (g)	11080	8030



Figure 30: Plug (left) and cavity (right) tools. The blackened areas are the wax remains after the production process

⁴ Sol: Colloidal silica, 40% wt suspension in H₂O. The Sol density was 1.3 Kg/lt

MuTool Final Report

Figures & Tables

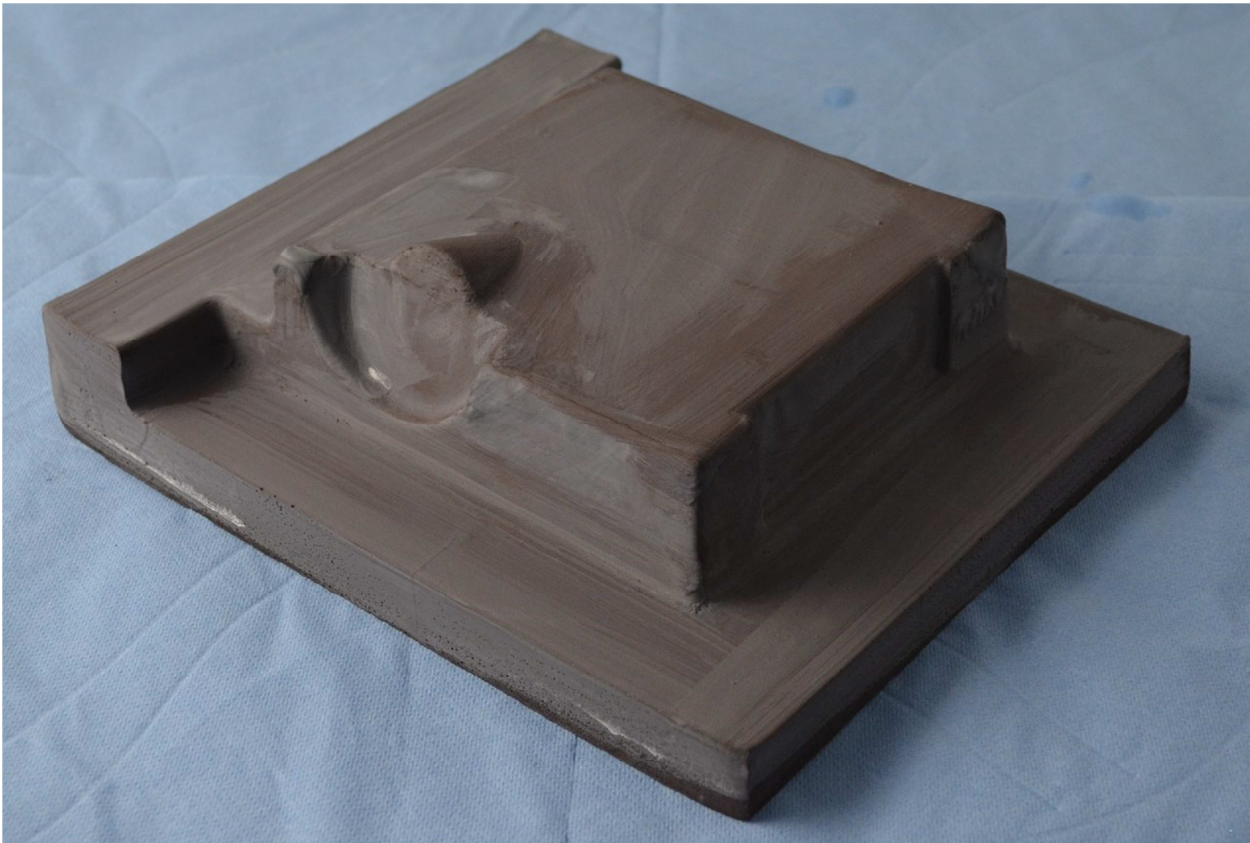


Figure 7: Cast Microcab demonstrator tool made of a cordierite/ferrite composite (70/30 vol%).

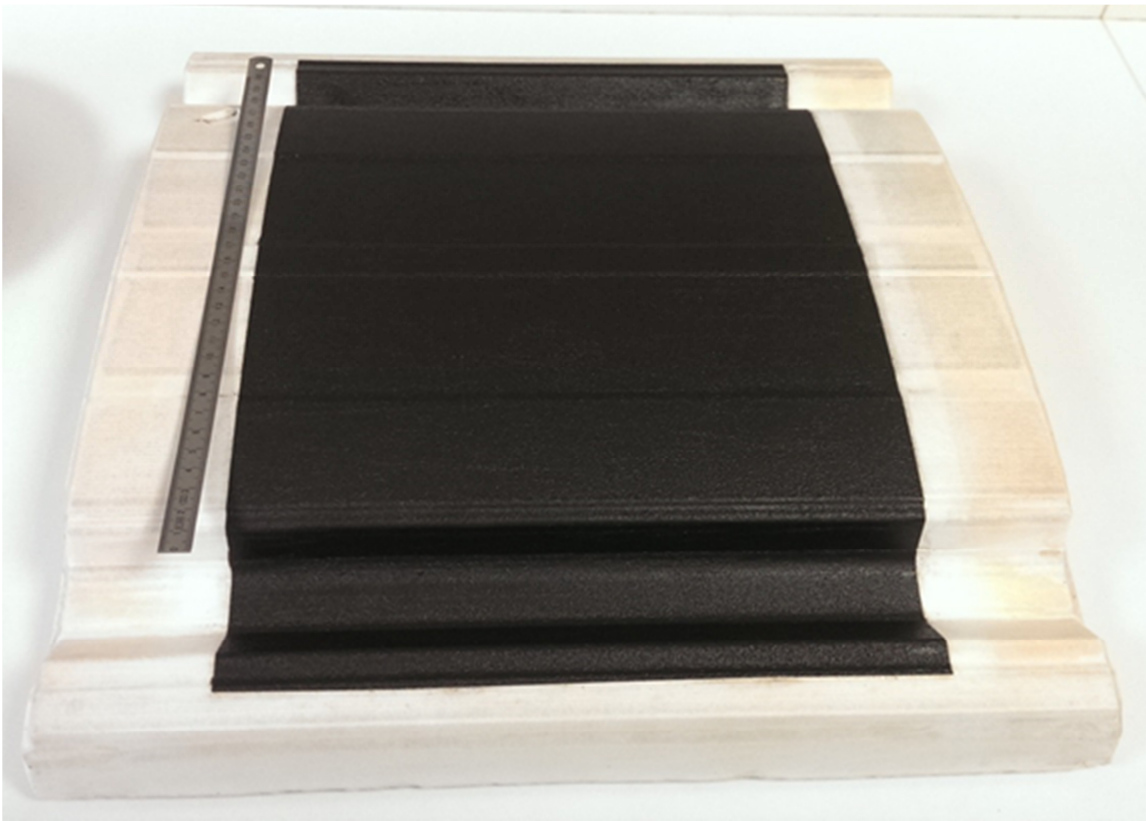


Figure 8: Final tool with the ferrite layer applied

MuTool Final Report

Figures & Tables

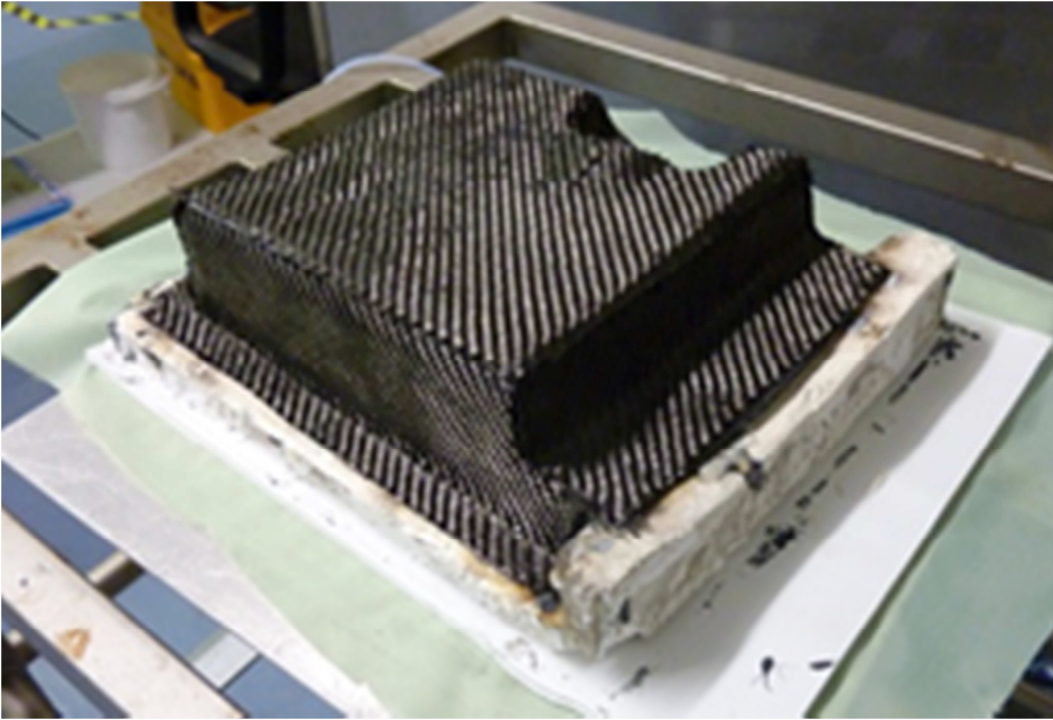


Figure 9: Hand layup of preform in the cavity tool



Figure 10: Final tool assembly prior to processing. Thermocouple probes can also be seen

MuTool Final Report

Figures & Tables

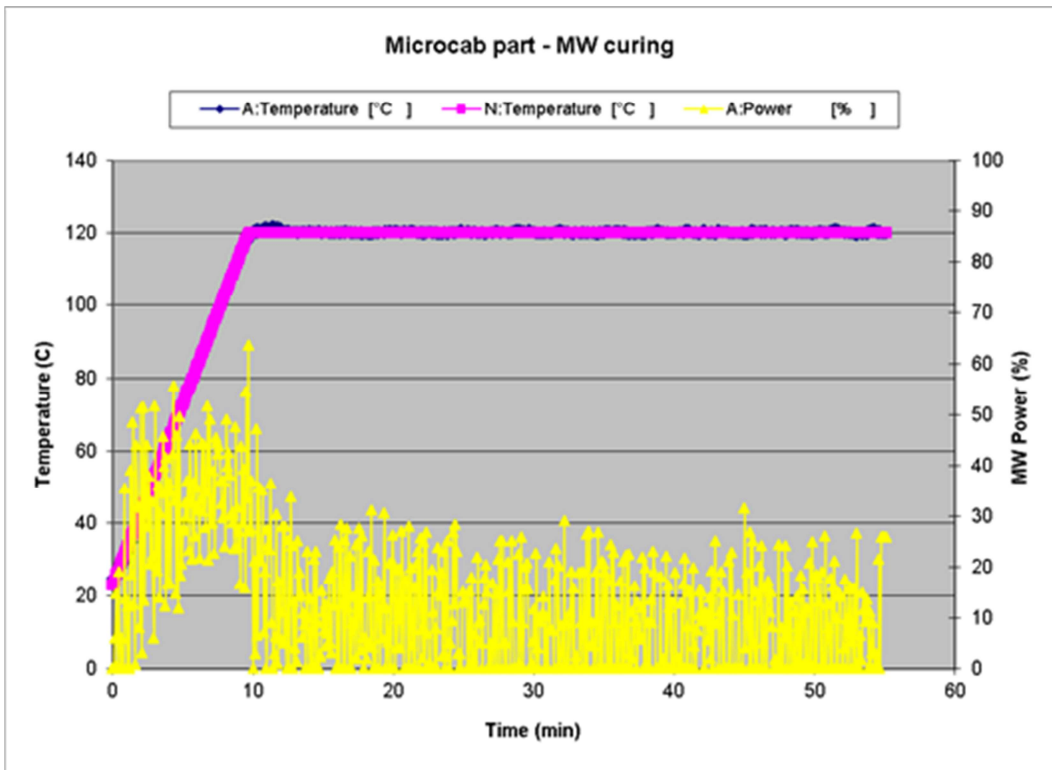


Figure 11: Temperature profile and MW power usage during the manufacturing of a carbon fibre composite part

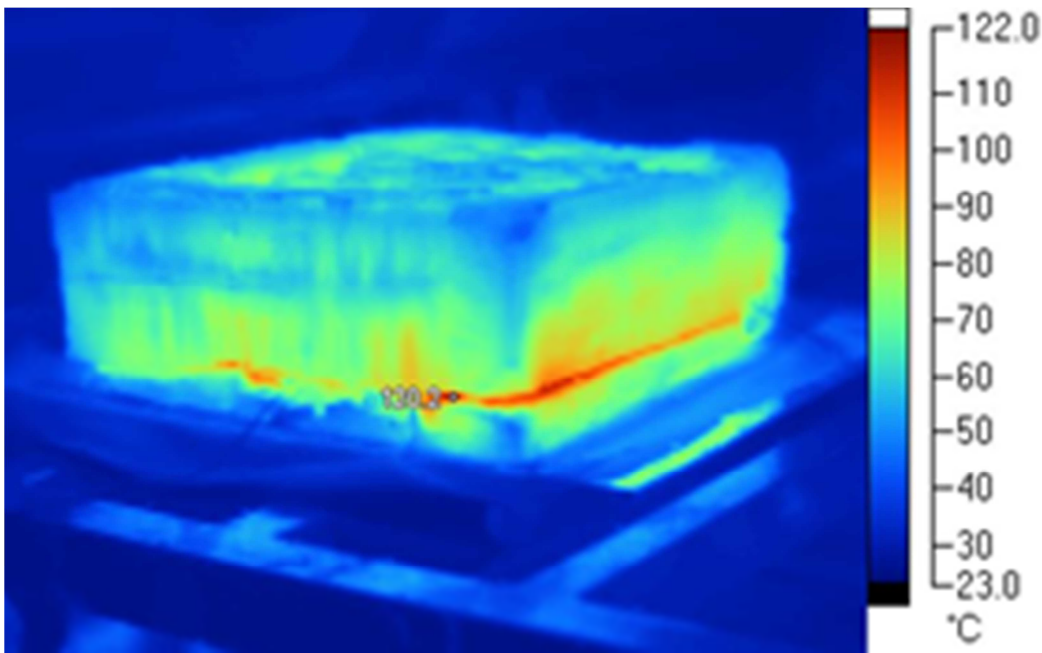


Figure 12: Thermal image of the tool right after the end of the curing process

MuTool Final Report

Figures & Tables

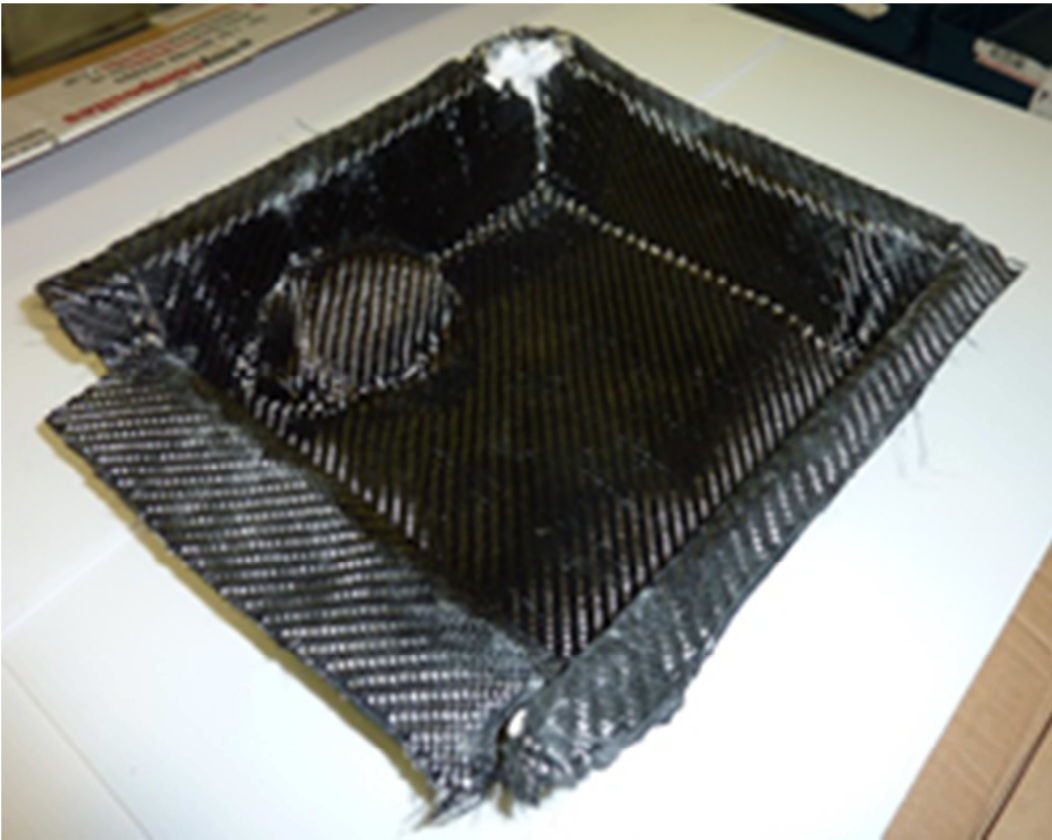


Figure 13: Cured carbon fibre composite

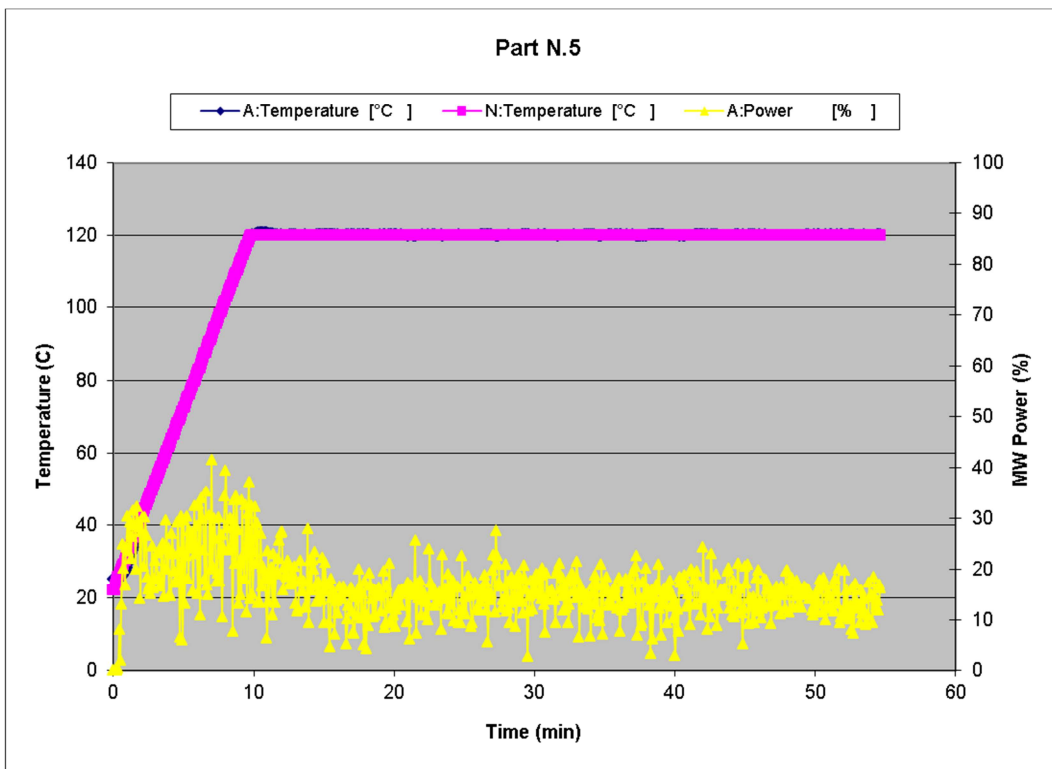


Figure 14: Temperature profile and MW power usage during the manufacturing of a glass fibre composite part

MuTool Final Report

Figures & Tables

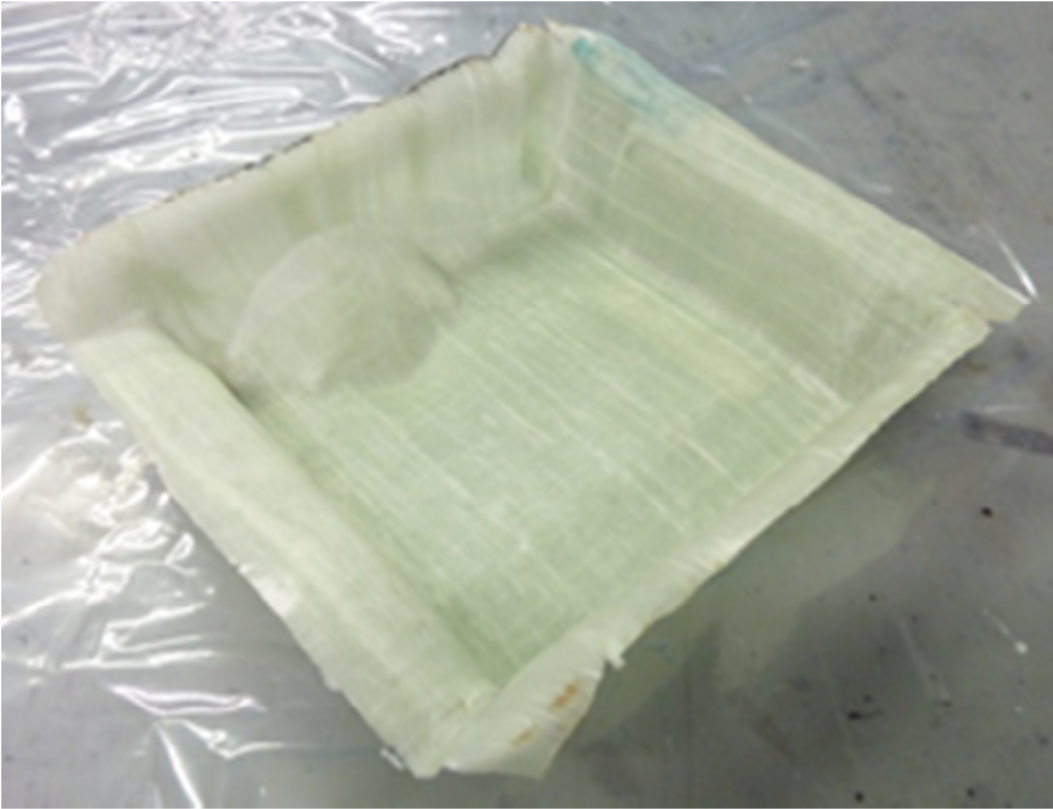


Figure 15: Cured glass fibre composite part



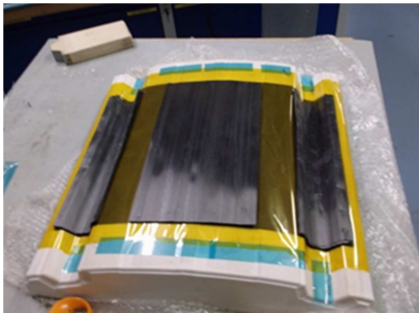
Figure 16: Demonstrator part drawing

MuTool Final Report

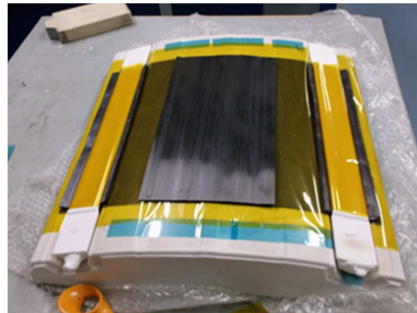
Figures & Tables



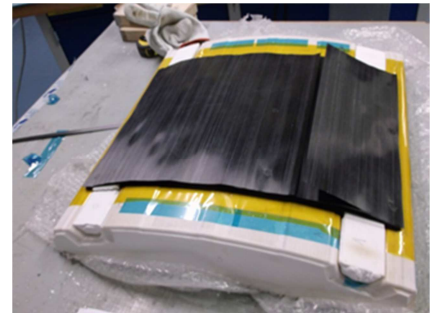
Figure 17: Carbon fibre PEEK prepreg being formed on the tool



(a)



(b)



(c)

Figure 42: (a) inner skin lay up composed of 11 plies, (b) cores wrapped in Kapton film and positioned on the tooling. (c) outer skin lay up composed of 11 plies

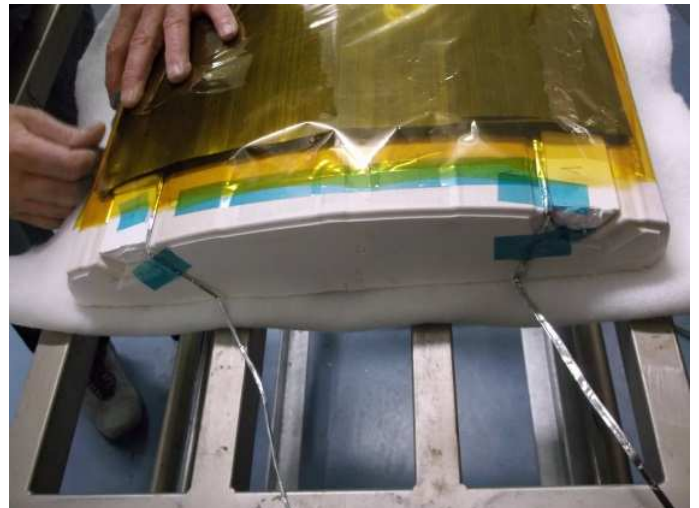
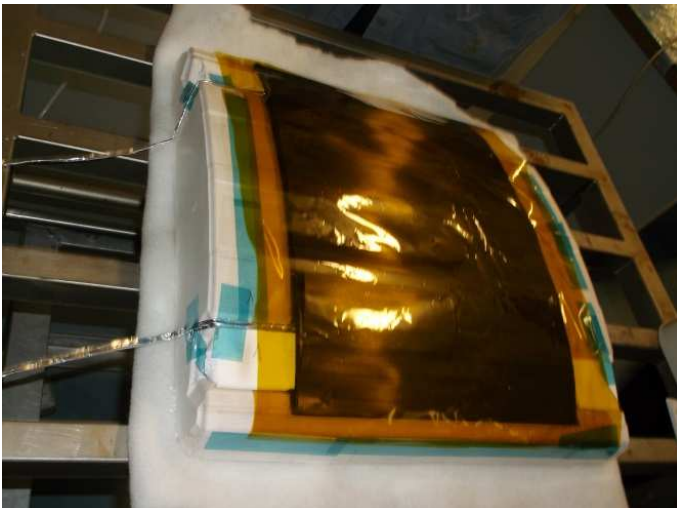


Figure 18: (a) Final composite lay-up and thermocouples positioned on the tooling (view from top on the left, view from side on the right). The orange Kapton® film can also be seen

MuTool Final Report

Figures & Tables



Figure 19: Tooling under vacuum and ready to be MW processed



Figure 20: Demonstrator 3 after being MW processed.

MuTool Final Report

Figures & Tables



Figure 21: LOIRETECH booth at JEC Paris 2014



Figure 22: Introductory slide of the slideshow presented at JEC Paris 2014

Table 2: Workforce statistics for the MUTOOL project

Type of position	Number of Women	Number of Men
Scientific coordinator	0	2
Work package leaders	1	3
Experienced researchers	2	15
PhD students	0	0
Other	1	1